
OpenSeg-R: Improving Open-Vocabulary Segmentation via Step-by-Step Visual Reasoning

Zongyan Han¹, Jiale Cao², Shuo Chen³, Tong Wang¹,
Jorma Laaksonen⁴, Rao Muhammad Anwer¹

¹Mohamed Bin Zayed University of Artificial Intelligence, Abu Dhabi, UAE

²Tianjin University, Tianjin, China ³Nanjing University, Nanjing, China

⁴Aalto University, Espoo, Finland

{zongyan.han, tong.wang, rao.anwer}@mbzuai.ac.ae

Abstract

Open-Vocabulary Segmentation (OVS) has drawn increasing attention for its capacity to generalize segmentation beyond predefined categories. However, existing methods typically predict segmentation masks with simple forward inference, lacking explicit reasoning and interpretability. This makes it challenging for OVS model to distinguish similar categories in open-world settings due to the lack of contextual understanding and discriminative visual cues. To address this limitation, we propose a step-by-step visual reasoning framework for open-vocabulary segmentation, named **OpenSeg-R**. The proposed OpenSeg-R leverages Large Multimodal Models (LMMs) to perform hierarchical visual reasoning before segmentation. Specifically, we generate both generic and image-specific reasoning for each image, forming structured triplets that explain the visual reason for objects in a coarse-to-fine manner. Based on these reasoning steps, we can compose detailed description prompts, and feed them to the segmentor to produce more accurate segmentation masks. To the best of our knowledge, OpenSeg-R is the first framework to introduce explicit step-by-step visual reasoning into OVS. Experimental results demonstrate that OpenSeg-R significantly outperforms state-of-the-art methods on open-vocabulary semantic segmentation across five benchmark datasets. Moreover, it achieves consistent gains across all metrics on open-vocabulary panoptic segmentation. Qualitative results further highlight the effectiveness of our reasoning-guided framework in improving both segmentation precision and interpretability. Our code is publicly available at <https://github.com/Hanzy1996/OpenSeg-R>.

1 Introduction

Image segmentation is a fine-grained visual recognition task that involves classifying every pixel in an image. This technique has been widely applied in domains such as autonomous driving [8, 30], medical imaging [4, 51], and remote scene [24, 36]. However, conventional segmentation methods are constrained by a predefined set of training classes, which limits their generalization ability to open-world. Open-Vocabulary Segmentation (OVS) [50, 39, 38] addresses this limitation by leveraging vision-language models such as CLIP [32] to enable segmentation beyond closed-set categories.

Current OVS approaches can be broadly categorized into two frameworks. The first employs a one-stage architecture [53, 40, 7], which computes similarity maps between image features and textual embeddings of class names via CLIP. These maps are then refined through upsampling or embedding transformations, followed by feature fusion to produce segmentation masks. The second category utilizes a two-stage framework [11, 22, 45, 18], initially generating class-agnostic mask proposals and subsequently aligning mask-specific features with text embeddings for semantic classification.

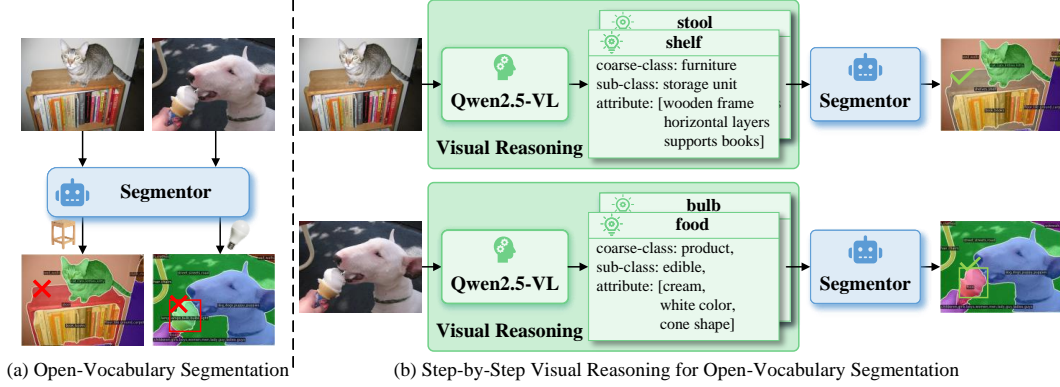


Figure 1: Comparison with open-vocabulary segmentor and our method. (a) Standard open-vocabulary segmentors struggle with visually or semantically similar categories. (b) Our OpenSeg-R guides the segmentor with hierarchical visual reasons, therefore generating accurate prediction.

Despite their success, these methods rely solely on associating class name with visual regions for segmentation, without any interpretable explanation or reasoning for segmentation outcomes. This lack of transparency undermines trust in model decisions and limits adaptability to some complex scenarios and difficult examples. For example, as illustrated in Fig. 1(a), an open-vocabulary segmentor incorrectly classifies a shelf as a stool due to their similar appearance and semantics.

To address this gap, we propose to improve open-vocabulary segmentation via step-by-step visual reasoning, named **OpenSeg-R**. It utilizes explicit visual cues and attributes to support segmentation. These cues offer more detailed and precise knowledge of the objects in the image, thereby enhancing both the accuracy and interpretability of the segmentation process.

Concretely, our framework mimics a human-like reasoning process using a Large Multimodal Model (LMM), such as Qwen2.5-VL [1]. The LMM is prompted to generate Image-Specific Reasoning, which begins by producing an overall description of the image and then identifying the presence of relevant object categories. Based on the observed classes, the LMM progressively explains the association between each object and its corresponding category through coarse-to-fine reasoning steps. As illustrated in Fig. 1(b), the hierarchical reasoning process first identifies the coarse and sub-category levels, which helps eliminate irrelevant distractor classes (e.g., distinguishing food from bulb). Subsequently, fine-grained attribute-based descriptions are used to disambiguate visually similar categories (e.g., shelf vs. stool).

To supplement categories that may be overlooked by the LMM, we further introduce a Generic Class Reasoning module. For each unobserved class, the LMM will generate a coarse-to-fine reason that highlights key features for distinguishing it from visually similar categories. We then feed both the image-specific and generic reasoning into the segmentor to perform open-vocabulary segmentation.

Our OpenSeg-R not only provides richer and more discriminative semantic context for improved segmentation performance, but also enhances model interpretability in open-world scenarios. We evaluate OpenSeg-R on open-vocabulary semantic segmentation across five benchmark datasets, and on open-vocabulary panoptic segmentation using a widely adopted benchmark. On both tasks, our method achieves state-of-the-art performance.

Our contributions can be summarized as below:

- We are the first to propose improving open-vocabulary segmentation through step-by-step visual reasoning. Our framework, OpenSeg-R, mimics human-like reasoning by leveraging a Large Multimodal Model (LMM).
- We introduce two complementary reasoning modules: Image-Specific Reasoning and Generic Class Reasoning, which improve both the accuracy and interpretability of segmentation.
- Our method achieves state-of-the-art results on five open-vocabulary semantic segmentation benchmarks and the popular open-vocabulary panoptic segmentation benchmark.

2 Related Work

2.1 Open-Vocabulary Segmentation

Open-vocabulary segmentation has emerged recently as its ability to segment unseen categories. Early efforts in this field focus on aligning visual features with pre-trained text embeddings through learned feature mappings [39, 3]. The introduction of large-scale vision-language models like CLIP [32] marked a turning point, empowering subsequent methods with strong zero-shot capabilities. Two major paradigms have since evolved: two-stage and single-stage frameworks. Two-stage methods [22, 11, 43, 15, 10, 14, 31] first generate class-agnostic mask proposals, then classify them using text embeddings. For example, OVSeg [22] fine-tunes CLIP on masked images paired with text annotations to enhance classification accuracy in the second stage. Similarly, MaskCLIP [11] incorporates mask tokens into the pre-trained CLIP model to refine masks and improve classification. While ODISE [43] uses a diffusion model for mask generation and CLIP-based features for recognition. In contrast, single-stage methods [20, 53, 48, 7, 18, 42, 29] directly align pixel-level features with CLIP’s text embeddings. LSeg [20] pioneers this direct alignment, while SAN [44] and FC-CLIP [48] enhance it with architectural refinements. Recent works like CAT-Seg [7] and SED [40] improve performance by aggregating cost maps spatially or across scales. Notably, CAT-Seg [7] further finetunes the CLIP model during training to better adapt it to the segmentation task. Further, MAFT [17] and MAFTPlus [18] explore text encoder fine-tuning strategies, introducing content-aware mechanisms to retain CLIP’s generalization while improving segmentation of novel categories.

2.2 Vision-Language Models

Visual-language models (VLMs) integrate visual and linguistic modalities to enable open-world visual understanding. Early VLMs [21, 27], trained on small multi-modal datasets, use task combinations for cross-modal alignment. The introduction of CLIP [32] marks a shift, utilizing large-scale image-text pairs and contrastive learning for direct alignment, while ALIGN [16] further scales datasets, embracing noisy data for diverse pretraining. Concurrently, large language models (LLMs) such as LLaMA [34] and QWen [46] have achieved remarkable success in language tasks, providing strong and adaptable foundations. Building on this progress, large multimodal models (LMMs) like LLaVA [25] and QWen-VL [1] have emerged, integrating visual encoders, pre-trained LLMs, and cross-modal alignment modules. Together, these developments have significantly advanced the open-world understanding capabilities of multimodal systems.

2.3 Step-by-Step Reasoning

To emulate human sequential reasoning, step-by-step techniques guide Large Language Models (LLMs) in producing structured reasoning steps. The Chain-of-Thought (CoT) [37] method enhances arithmetic reasoning but relies on manually crafted prompts. To overcome this limitation, Auto-CoT [49] automates demonstration creation with questions and reasoning chains. Building on this, Tree-of-Thoughts (ToT) [47] enables LLMs to explore multiple reasoning pathways for flexible decision-making. Further advancing the field, Graph-of-Thoughts (GoT) [2] models information as a graph, with units as vertices and relationships as edges. Despite these advances, all methods maintain a sequential decoding approach, directing LLMs to reason step-by-step.

Although recent open-vocabulary segmentation methods have achieved remarkable progress, they still struggle to distinguish objects with similar appearance or semantic meaning. We propose Step-by-Step Visual Reasoning for Open-Vocabulary Segmentation, a framework that guides the segmentation process through interpretable, hierarchical visual explanations via LMMs.

3 Method

3.1 Preliminary: Open-Vocabulary Segmentor

An open-vocabulary segmentor \mathbf{A} is designed to perform segmentation on images that may contain arbitrary, potentially unseen object categories, despite being trained on a fixed set of classes. Given an input image $\mathbf{o} \in \mathbb{R}^{H \times W \times 3}$ and a target class $c \in \mathcal{C}$, where \mathcal{C} is an open-ended or user-defined set of class names, the goal of the segmentor is to produce a segmentation mask \mathbf{m}_c that highlights

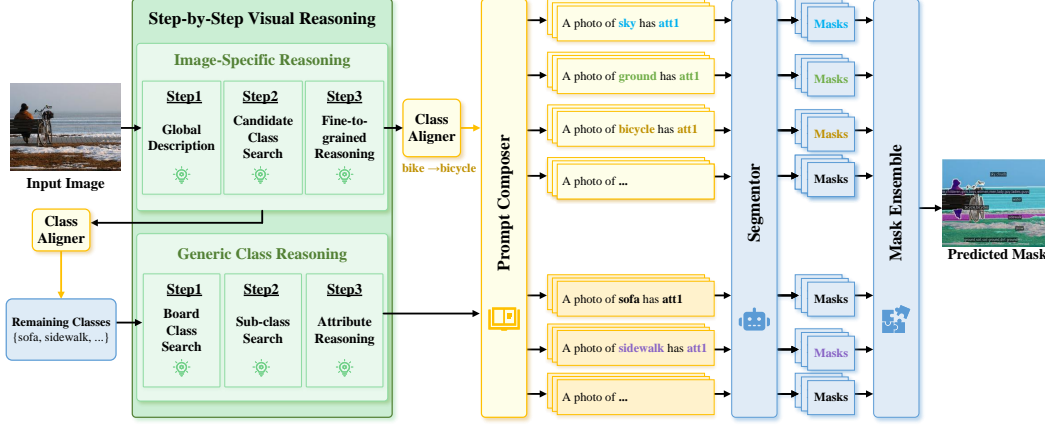


Figure 2: The whole framework of our **OpenSeg-R**. We first use an LMM to generate image-specific reasoning in a step-by-step manner. Predicted classes are aligned to the predefined label set via a class aligner. For unobserved classes, the LMM generates generic coarse-to-fine reasoning. All reasoning results are composed into prompts and fed to the segmentor to produce masks, which are then aggregated into the final prediction.

regions in the image corresponding to class c . To achieve this, the class name c is first converted into a textual prompt p_c (e.g., ‘a photo of a $\{c\}$ ’) using a prompt composer P . This prompt is then embedded into a joint visual-semantic space using a vision-language model such as CLIP [32]. Subsequently, the segmentor S integrates the text embedding with image features to generate the class-specific mask prediction. Formally, this process can be formulated as:

$$\mathbf{m}_c = S(\mathbf{o}, \text{CLIP}(\mathcal{P}_c)), \quad \mathcal{P}_c = P(c), \quad c \in \mathcal{C}, \quad (1)$$

where \mathbf{m}_c denotes the predicted binary mask corresponding to class c .

This design allows the segmentor to generalize beyond training classes by conditioning on arbitrary class names. However, it still suffers struggles in complex scenarios, such as distinguishing between visually or semantically similar objects. To address these limitations, we propose a Step-by-Step Visual Reasoning framework for Open-Vocabulary Segmentation (**OpenSeg-R**).

3.2 Step-by-Step Visual Reasoning

As shown in Fig. 2, our **OpenSeg-R** first performs step-by-step visual reasoning to generate image-specific reasoning. Next, we apply a *Class Aligner* to map the class names predicted by the LMM back to the original class set. To complement missing categories, we further introduce *Generic Class Reasoning*. The combined reasoning outputs are then passed to the *Prompt Composer* and *Segmentor*, followed by mask ensembling to produce the final segmentation results. We provide a detailed illustration of each component in the following sections.

3.2.1 Image-Specific Reasoning

Instead of directly feeding the image and candidate class set into the segmentor, we first prompt a large multimodal model (LMM), such as Qwen2.5-VL [1], to perform a step-by-step analysis of the visual content. Concretely, the reasoning process consists of three steps. **Step 1**: the LMM generates a high-level description of the input image, capturing its overall context and salient content. This step ensures that the model builds a global understanding of the scene before performing object-level reasoning. **Step 2**: conditioned on this description and the image, the LMM identifies which classes from the class set \mathcal{C} are present in the scene, yielding a filtered subset \mathcal{C}_o . This step selects candidate classes, providing the foundation for generating fine-grained class-specific reasoning in the next stage. **Step 3**, for each identified class in \mathcal{C}_o , the LMM generates a coarse-to-fine reason that justifies its

presence in the image. This process can be formalized as:

$$\mathcal{T}_o = (\mathbf{o}, \mathcal{C}_o, \mathcal{R}_o), \quad \text{where} \quad \begin{cases} \mathcal{D} = \text{LMM}(\mathbf{o}), \\ \mathcal{C}_o = \text{LMM}(\mathbf{o}, \mathcal{D}, \mathcal{C}), \\ \mathcal{R}_o = \text{LMM}(\mathbf{o}, \mathcal{C}_o). \end{cases} \quad (2)$$

\mathcal{T}_o is the image-specific reasoning triplet, \mathcal{D} denotes the overall image description, \mathcal{C}_o is the subset of classes observed in the image, and \mathcal{R}_o contains the corresponding reasoning outputs for each class in \mathcal{C}_o . For each image, the reasoning result is organized as a triplet $(\mathbf{o}, \mathcal{C}_o, \mathcal{R}_o)$.

Notably, our OpenSeg-R benefits from the step-by-step strategy, as it decomposes the task into manageable sub-problems, making it easier for the LMM to understand and reason effectively. Furthermore, the coarse-to-fine reasoning process begins with broad categories (e.g., living being), narrows down to subcategories (e.g., animal), and finally identifies the most discriminative semantic attributes (e.g., four legs). This progressive structure helps the model highlight distinguishing features, enabling it to better differentiate the target class from other visually or semantically similar categories.

3.2.2 Class Aligner

Due to the limited context retention and instruction-following consistency of LMMs, the predicted class names may not always exactly match the original input class set. To address this issue and provide more reliable guidance to the segmentor, we introduce a Class Aligner module that maps the class names generated by the LMM back to the original predefined class set. Concretely, for class names c_u that are not defined in the original class set \mathcal{C} , we employ Sentence Transformers [33] (denoted as SenTF) to perform semantic alignment. Specifically, we first encode the LMM-predicted class c_u and all candidate classes $c \in \mathcal{C}$ using SenTF, and compute their pairwise cosine similarity. We then select the most semantically similar class c_r from the original class set as the matched class:

$$c_r = \arg \max_{c \in \mathcal{C}} \cos [\text{SenTF}(c_u), \text{SenTF}(c)], c_u \in \mathcal{C}_o, c_u \notin \mathcal{C}, \quad (3)$$

where $\cos[\cdot]$ denotes the cosine similarity between the SenTF embeddings. We further introduce a similarity threshold σ to ensure reliable replacement. If the maximum similarity score exceeds σ , we treat c_r as the aligned class for c_u ; otherwise, c_u is considered unmatched and discarded from subsequent segmentation:

$$\hat{c}_u = \begin{cases} c_r, & \text{if } \cos [\text{SenTF}(c_u), \text{SenTF}(c_r)] > \sigma; \\ \emptyset, & \text{otherwise.} \end{cases} \quad (4)$$

After this alignment step, we obtain the semantic aligned image-specific reasoning triplet:

$$\hat{\mathcal{T}}_o = (\mathbf{o}, \hat{\mathcal{C}}_o, \hat{\mathcal{R}}_o), \quad (5)$$

where $\hat{\mathcal{C}}_o$ is the filtered set of matched classes and $\hat{\mathcal{R}}_o$ contains the corresponding reasoning outputs. This alignment process ensures consistency between the LMM’s generated outputs and the segmentor’s required inputs, thereby improving both the accuracy and robustness of downstream open-vocabulary segmentation.

Although the LMM can recognize most salient objects, it may overlook classes that occupy small regions or have low visual prominence —such as the ‘sidewalk’ in Fig. 2. In addition, when the candidate class list is too long, the LMM may ignore certain valid classes due to its limited context length and attention capacity. Such omissions can result in incomplete or biased segmentation outcomes. To address this issue, we introduce a Generic Class Reasoning module as a complementary component to the image-specific reasoning.

3.2.3 Generic Class Reason

For the classes $c_g \notin \hat{\mathcal{C}}_o$, that was not detected by the LMM, we further prompt the LMM to provide a generic explanation describing how this class is visually distinguishable from others. This reasoning is also structured in a coarse-to-fine manner, starting from broad category distinctions and progressively focusing on discriminative fine-grained visual attributes. After that, we obtain the generic class reasoning triplet:

$$\mathcal{T}_g = (\mathbf{o}, \mathcal{C}_g, \mathcal{R}_g), \quad (6)$$

where \mathcal{C}_g denotes the set of candidate classes that were not detected in the image-specific reasoning (i.e., $\mathcal{C}_g = \mathcal{C} \setminus \hat{\mathcal{C}}_o$), and \mathcal{R}_g contains the corresponding generic reasoning outputs generated by the LMM for each class in \mathcal{C}_g .

Overall, the final reasoning instruction is constructed by integrating both the image-specific and the generic class Reasoning components:

$$\mathcal{T} = (\mathbf{o}, \mathcal{C}, \mathcal{R}) = (\mathbf{o}, \hat{\mathcal{C}}_o \cup \mathcal{C}_g, \hat{\mathcal{R}}_o \cup \mathcal{R}_g). \quad (7)$$

With visual reasoning triplet \mathcal{T} , which encodes rich semantic and structural information, we then feed it into the segmentor to generate the corresponding segmentation masks.

3.3 Mask Generation

Prompt Composer We employ a reason prompt composer P_r to convert each class-reason pair from \mathcal{T} into a descriptive textual prompt for the segmentor. Unlike traditional prompts that consist only of class names (e.g., ‘a photo of $\{c\}$ ’), our P_r incorporates the associated reasoning to enrich semantic guidance. Specifically, for each pair (c, r) , we use a compositional template such as ‘a photo of $\{c\}$ has $\{r\}$ ’ to construct the final prompt. Formally, the composed prompts are generated as:

$$\mathcal{P}_c = P_r(c, \mathcal{R}_c), \quad c \in \mathcal{C}, \quad (8)$$

where \mathcal{P}_c denotes the prompt set for class c using its corresponding reasoning \mathcal{R}_c .

Reason-Guided Mask Following standard segmentor [18, 40], we use CLIP [32] to embed the reason-based prompts as text embeddings. These embeddings are then fed into the segmentor S alongside the input image to generate reason-guided segmentation masks:

$$\mathbf{m}_c^r = S(\mathbf{o}, \text{CLIP}(\mathcal{P}_c)), \quad \mathbf{m}_c^r \in \mathbb{R}^{N \times H \times W}, \quad (9)$$

where \mathbf{m}_c^r denotes the set of predicted masks for class c , guided by the corresponding reason-based prompts \mathcal{P}_c , and N is the number of reasons associated with class c .

Mask Ensemble To obtain a single unified binary mask for each class, we aggregate the multiple reason-guided masks using average pooling, followed by a sigmoid activation and thresholding. For each class c , the final binary segmentation mask is computed as:

$$\bar{\mathbf{m}}_c = \mathbb{I} \left[\sigma \left(\frac{1}{N} \sum_{i=1}^N \mathbf{m}_c^{r_i} \right) > \tau \right], \quad (10)$$

where $\mathbf{m}_c^{r_i} \in \mathbb{R}^{H \times W}$ is the predicted mask from the i -th reasoning prompt, $\sigma(\cdot)$ denotes the sigmoid function, τ is a predefined binarization threshold, $\mathbb{I}[\cdot]$ is the indicator function, and $\bar{\mathbf{m}}_c \in \mathbb{R}^{H \times W}$ is the final binary segmentation mask, obtained by aggregating the reasoning knowledge associated with the class.

The final predicted mask is inferred based on the visual reasoning generated by the LLM. This process ensures that segmentation is guided by interpretable, fine-grained visual cues, leading to more precise and semantically aligned predictions.

4 Experiments

4.1 Datasets and Evaluation Metric

Datasets Following prior works [7, 44, 6, 43, 18], we train OpenSeg-R on COCO-Stuff [5] and COCO-Panoptic [23]. COCO-Stuff provides 164,000 images with semantic annotations across 171 categories, while COCO-Panoptic offers panoptic annotations over the same image set for 133 categories. We use the full training splits of both datasets. To evaluate OpenSeg-R, we test it across several widely-used benchmarks, including ADE20K [52] (A-150 and A-847), PASCAL VOC [12] (PAS-20), and PASCAL-Context [28] (PC-59 and PC-459), covering a wide spectrum of categories and scene complexities. ADE20K includes 20,000 training images and supports both 150-category and 847-category open-vocabulary splits. PASCAL-Context extends PASCAL VOC with 4,998

Table 1: Comparison with state-of-the-art methods on open-vocabulary *semantic* segmentation. “**OpenSeg-R w/**” indicates our method combined with the corresponding segmentor. The results with improvements are marked in bold.

Method	VLM	A-847	PC-459	A-150	PC-59	PAS-20
SPNet [39]	-	-	-	-	24.3	18.3
ZS3Net [3]	-	-	-	-	19.4	38.3
LSeg [20]	ViT-B/32	-	-	-	-	47.4
LSeg+ [13]	ALIGN	2.5	5.2	13.0	36.0	-
Han et al. [15]	ViT-B/16	3.5	7.1	18.8	45.2	83.2
GroupViT [42]	ViT-S/16	4.3	4.9	10.6	25.9	50.7
ZegFormer [10]	ViT-B/16	4.9	9.1	16.9	42.8	86.2
SimBaseline [45]	ViT-B/16	7.0	-	20.5	47.7	88.4
OpenSeg [13]	ALIGN	4.4	7.9	17.5	40.1	-
DeOP [14]	ViT-B/16	7.1	9.4	22.9	48.8	91.7
PACL [29]	ViT-B/16	-	-	31.4	50.1	72.3
OVSeg [22]	ViT-B/16	7.1	11.0	24.8	53.3	92.6
SAN [44]	ViT-B/16	10.1	12.6	27.5	53.8	94.0
CAT-Seg [7]	ViT-B/16	12.0	19.0	31.8	57.5	94.6
SCAN [26]	ViT-B/16	10.8	13.2	30.8	58.4	97.0
SED [40]	ConvNeXt-B	11.4	18.6	31.6	57.3	94.4
OpenSeg-R w SED	ConvNeXt-B	11.8	18.9	33.6	59.0	95.1
MAFT+ [18]	ConvNeXt-B	13.8	14.6	34.6	57.5	95.4
OpenSeg-R w MAFT+	ConvNeXt-B	15.2	15.5	35.5	59.0	96.1
LSeg [20]	ViT-L/14	-	-	-	-	52.3
OpenSeg [13]	ALIGN	8.1	11.5	26.4	44.8	-
OVSeg [22]	ViT-L/14	9.0	12.4	29.6	55.7	94.5
Ding <i>et al.</i> [11]	ViT-L/14	8.2	10.0	23.7	45.9	-
ODISE [43]	ViT-L/14	11.1	14.5	29.9	57.3	-
HIPIE [35]	BERT-B [9]	-	-	29.0	59.3	-
SAN [44]	ViT-L/14	13.7	17.1	33.3	60.2	95.5
FC-CLIP [48]	ConvNeXt-L	14.8	18.2	34.1	58.4	95.4
CAT-Seg [7]	ViT-L/14	16.0	23.8	37.9	63.3	97.0
SCAN [26]	ViT-L/14	14.0	16.7	33.5	59.3	97.2
SED [40]	ConvNeXt-L	13.9	22.6	35.2	60.6	96.1
OpenSeg-R w SED	ConvNeXt-L	14.3	22.0	36.1	61.2	96.3
MAFT+ [18]	ConvNeXt-L	15.3	16.7	36.2	59.5	96.4
OpenSeg-R w MAFT+	ConvNeXt-L	16.8	17.1	37.1	60.3	96.2

training and 5,005 validation images, and defines PC-59 and PC-459 as open-vocabulary test sets. PASCAL VOC itself contains 20 object categories with augmented annotations for segmentation. Beyond semantic segmentation, we further validate OpenSeg-R in the open-vocabulary panoptic segmentation setting [6, 43], evaluating on ADE20K to demonstrate its versatility across tasks.

Evaluation Metric Following standard practices in traditional and open-vocabulary semantic segmentation [10, 22, 6, 43], we use mean Intersection over Union (mIoU), calculated as the average intersection over union across all classes, to quantitatively evaluate semantic segmentation performance. For panoptic segmentation, we adopt Panoptic Quality (PQ), Segmentation Quality (SQ), and Recognition Quality (RQ) as evaluation metrics.

4.2 Implementation Details

We use Qwen2.5-VL-72B-Instruct-AWQ [1] to process input images and generate step-by-step reasoning outputs, running on 2 A100 GPUs. The detailed inference prompts are provided in the supplementary material. In the Prompt Composer, we use descriptive attributes as reasoning outputs and combine them with class names to construct prompts for mask generation. For class name alignment, we employ all-MiniLM-L6-v2 from Sentence Transformers[33], using a similarity threshold of $\sigma = 0.5$. τ is also set to 0.5. Since the PAS-20 dataset contains relatively few candidate classes, the LMM can reliably identify all relevant categories; thus, we omit generic reasoning for this dataset. We adopt both SED [40] and MAFT+ [18] as our segmentors, each evaluated using 4 A100 GPUs. For open-vocabulary semantic segmentation, both models are pretrained on COCO-Stuff [5]. For panoptic segmentation, MAFT+ is pretrained on COCO-Panoptic [23].

Table 2: Open-vocabulary *panoptic* segmentation performance on ADE20K. PQ, SQ, and RQ are used for evaluation. The best results are highlighted with **bold**.

Method	PQ	SQ	RQ
FreeSeg [31]	16.3	-	-
ODISE [43]	22.6	-	-
MaskCLIP [11]	15.1	70.4	19.2
OPNet [6]	19.0	52.4	23.0
FC-CLIP [48]	21.9	71.5	26.4
FC-CLIP* [48]	26.8	71.5	32.2
MAFT+ [18]	27.1	73.5	32.9
OpenSeg-R w MAFT+	28.0	75.0	34.2

Table 3: Effect of different prompt choices on open-vocabulary segmentation.

Method	Prompt Type	VLM	A-847	PC-459	A-150	PC-59	PAS-20
MAFT+ [18]	Class name	ConvNeXt-B	13.8	14.6	34.6	57.5	95.4
OpenSeg-R w MAFT+	Coarse	ConvNeXt-B	13.4	14.3	34.1	57.2	95.8
OpenSeg-R w MAFT+	Coarse + Att	ConvNeXt-B	15.1	15.4	35.3	59.0	95.9
OpenSeg-R w MAFT+	Att	ConvNeXt-B	15.2	15.5	35.5	59.0	96.1
MAFT+ [18]	Class name	ConvNeXt-L	15.3	16.7	36.2	59.5	96.4
OpenSeg-R w MAFT+	Coarse	ConvNeXt-L	15.1	16.8	35.8	59.2	96.3
OpenSeg-R w MAFT+	Coarse + Att	ConvNeXt-L	16.7	17.4	36.7	60.0	96.3
OpenSeg-R w MAFT+	Att	ConvNeXt-L	16.8	17.1	37.1	60.3	96.2

4.3 Comparison with State-of-the-arts

Open-Vocabulary Semantic Segmentation We compare our method with state-of-the-art approaches on open-vocabulary *semantic* segmentation, as shown in Tab. 1. Among them, SED [40] and MAFT+ [18] are representative one-stage and two-stage segmentation frameworks, respectively. We integrate our reasoning module into both architectures, resulting in two variants: **OpenSeg-R** w/ SED and **OpenSeg-R** w/ MAFT+. With a relatively small vision-language model (VLM), our method consistently outperforms the corresponding baselines across all benchmarks. The proposed **Open-OpenSeg-R** variants achieve the best results in all settings. Specifically, on A-150, our method yields an improvement of approximately **2%** when integrated with SED [40]. On A-847, which contains more fine-grained categories than A-150, **OpenSeg-R** w/ MAFT+ achieves a **1.7%** gain over MAFT+ [18], surpassing or matching the performance of methods that utilize significantly larger VLMs. A similar trend is observed on PAS-20, further demonstrating the effectiveness and generalization ability of our reasoning-enhanced framework. Our method surpasses all SOTA methods on A-150, A-847, and PC-459.

When using larger VLM, our method achieves further improvements across all datasets. However, the relative gains are smaller compared to that with the smaller VLM. On PC-459 with SED [40] and PAS-20 with MAFT+ [18], we even observe a slight performance drop. This may be attributed to that larger VLMs tend to produce category-level and generic text embeddings, which can suppress attribute-level cues. Similar issues have been observed in prior work [19, 41]. We also find that CAT-Seg [7] is not well-suited for our OpenSeg-R, as its finetuning of CLIP disrupts the visual-semantic space, making it less compatible with our detailed visual reasoning.

Open-Vocabulary Panoptic Segmentation In Tab. 2, we compare our method on the open-vocabulary *panoptic* segmentation task. Once again, our approach achieves consistent improvements across all evaluation metrics and outperforms all baselines. Specifically, it brings a gain of **0.9%** in Panoptic Quality (PQ), **2.3%** in Segmentation Quality (SQ), and **1.3%** in Recognition Quality (RQ). These results demonstrate the effectiveness of our reasoning-guided framework in enhancing both semantic understanding and instance-level discrimination in open-vocabulary scenarios.

4.4 Ablation Study

Prompt Type The reasoning output consists of three components: broad class, sub-class, and fine-grained visual attributes. Based on these, we construct four types of prompts: (1) *class name only* (baseline), (2) *coarse reason* (broad + sub-class), (3) *coarse + attribute*, and (4) *attribute only*. As shown in Tab. 3, using coarse reasoning alone slightly degrades performance, as such descriptions (e.g., ‘a dog that is an animal’) are too generic to distinguish similar categories. In contrast, incorporating fine-grained attributes consistently improves results across all datasets. Notably, prompts using

Table 4: Comparison of different reasoning types using MAFT+ as the segmentor.

Reason	VLM	A-847	PC-459	A-150	PC-59	PAS-20
Generic class	ConvNeXt-B	14.0	13.6	33.4	57.3	95.8
Image-specific	ConvNeXt-B	13.3	15.4	35.2	58.7	96.1
Both	ConvNeXt-B	15.2	15.5	35.5	58.9	95.1
Generic class	ConvNeXt-L	16.0	15.5	35.5	59.2	95.5
Image-specific	ConvNeXt-L	14.0	15.7	35.9	59.3	96.2
Both	ConvNeXt-L	16.8	17.1	37.1	60.3	95.8

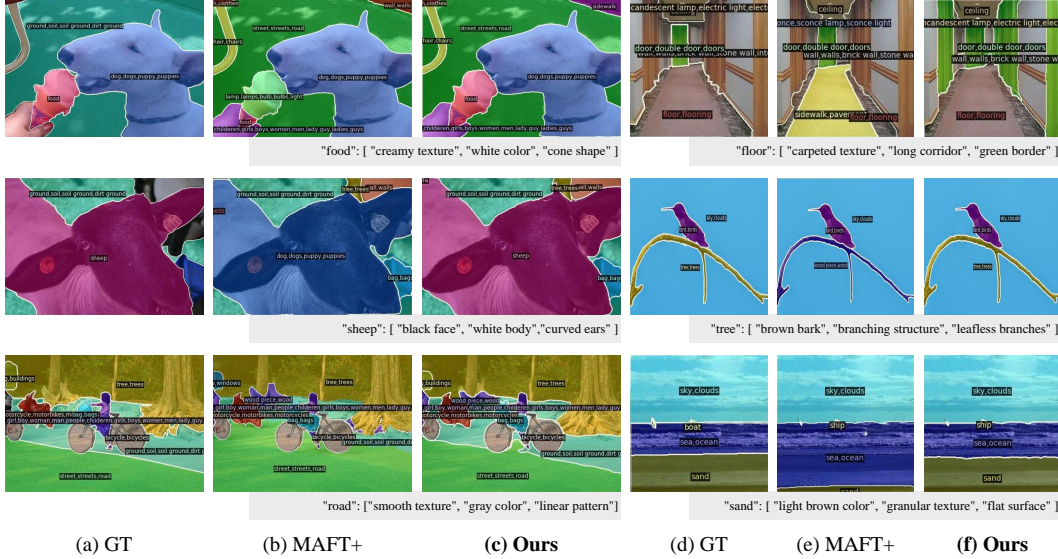


Figure 3: Qualitative comparison with MAFT+ [18] on open-vocabulary semantic segmentation. We highlight the visual reasoning behind the class that is missed by MAFT, demonstrating how our method recovers it through step-by-step visual reasoning.

attributes alone achieve the best performance in most cases, suggesting that detailed visual cues provide the most discriminative and informative guidance for open-vocabulary segmentation.

Reason Type We evaluate the effectiveness of different reasoning types in Tab. 4, comparing three configurations: (1) generic class reasoning only, (2) image-specific reasoning only, and (3) their combination. Generic reasoning performs worse across most datasets, as its descriptions are often too broad to distinguish visually similar objects, leading to lower segmentation accuracy. In contrast, image-specific reasoning, which is inferred from image content, provides more discriminative cues and achieves better performance. However, LMMs may still overlook certain objects. By combining both reasoning types, our method compensates for such omissions: generic reasoning recovers missed categories, while image-specific reasoning improves class-level discrimination. As shown in the table, this hybrid approach yields the best overall results. For PAS-20, which contains relatively few and easily recognizable categories, image-specific reasoning alone is sufficient, as the LMM can reliably detect all relevant classes without generic supplementation.

4.5 Qualitative Results

To further illustrate the effectiveness of our method, we present qualitative comparisons in Fig. 3. We present several cases where baseline methods MAFT+ [18] fail to correctly segment or classify objects due to ambiguous visual or semantic cues. For each case, we show the visual reasoning attributes inferred by the LMM. These reasoning cues help disambiguate visually similar categories and guide the segmentor toward more accurate predictions. As shown, our method produces more semantically aligned masks across a variety of categories, such as floor, tree, road, and sand, demonstrating the benefit of our OpenSeg-R in open-vocabulary segmentation.

5 Conclusion

In this paper, we introduce a novel method **OpenSeg-R** that improves open-vocabulary segmentation through step-by-step visual reasoning. OpenSeg-R leverages Large Multimodal Models (LMMs) to perform hierarchical reasoning based on the input image, generating both image-specific and generic class explanations, which are then composed into descriptive prompts to guide segmentation. Experiments on open-vocabulary semantic and panoptic segmentation benchmarks demonstrate the effectiveness and broad applicability of our approach.

References

- [1] Shuai Bai, Keqin Chen, Xuejing Liu, Jialin Wang, Wenbin Ge, Sibao Song, Kai Dang, Peng Wang, Shijie Wang, Jun Tang, Humen Zhong, Yuanzhi Zhu, Mingkun Yang, Zhaohai Li, Jianqiang Wan, Pengfei Wang, Wei Ding, Zheren Fu, Yiheng Xu, Jiabo Ye, Xi Zhang, Tianbao Xie, Zesen Cheng, Hang Zhang, Zhibo Yang, Haiyang Xu, and Junyang Lin. Qwen2.5-vl technical report. *arXiv preprint arXiv:2502.13923*, 2025.
- [2] Maciej Besta, Nils Blach, Aleš Kubíček, Robert Gerstenberger, Lukas Gianinazzi, Joanna Gajda, Tomasz Lehmann, Michal Podstawski, Hubert Niewiadomski, Piotr Nyczyk, and Torsten Hoefler. Graph of thoughts: Solving elaborate problems with large language models. In *AAAI Conference on Artificial Intelligence*, 2023.
- [3] Maxime Bucher, Tuan-Hung Vu, Matthieu Cord, and Patrick Pérez. Zero-shot semantic segmentation. In *Advances in Neural Information Processing Systems*, volume 32, pages 468–479, 2019.
- [4] Victor Ion Butoi, Jose Javier Gonzalez Ortiz, Tianyu Ma, Mert R Sabuncu, John Gutttag, and Adrian V Dalca. Universeg: Universal medical image segmentation. In *Proceedings of the IEEE/CVF International Conference on Computer Vision*, pages 21438–21451, 2023.
- [5] Holger Caesar, Jasper Uijlings, and Vittorio Ferrari. Coco-stuff: Thing and stuff classes in context. In *IEEE/CVF Conference on Computer Vision and Pattern Recognition*, pages 1209–1218, 2018.
- [6] Xi Chen, Shuang Li, Ser-Nam Lim, Antonio Torralba, and Hengshuang Zhao. Open-vocabulary panoptic segmentation with embedding modulation. *arXiv preprint arXiv:2303.11324*, 2023.
- [7] Seokju Cho, Heeseong Shin, Sunghwan Hong, Anurag Arnab, Paul Hongsuck Seo, and Seungryong Kim. Cat-seg: Cost aggregation for open-vocabulary semantic segmentation. In *Proceedings of the IEEE/CVF Conference on Computer Vision and Pattern Recognition*, pages 4113–4123, 2024.
- [8] Marius Cordts, Mohamed Omran, Sebastian Ramos, Timo Rehfeld, Markus Enzweiler, Rodrigo Benenson, Uwe Franke, Stefan Roth, and Bernt Schiele. The cityscapes dataset for semantic urban scene understanding. In *Proceedings of the IEEE conference on computer vision and pattern recognition*, pages 3213–3223, 2016.
- [9] Jacob Devlin, Ming-Wei Chang, Kenton Lee, and Kristina Toutanova. Bert: Pre-training of deep bidirectional transformers for language understanding. *arXiv preprint arXiv:1810.04805*, 2018.
- [10] Jian Ding, Nan Xue, Gui-Song Xia, and Dengxin Dai. Decoupling zero-shot semantic segmentation. In *IEEE/CVF Conference on Computer Vision and Pattern Recognition*, pages 11583–11592, 2022.
- [11] Zheng Ding, Jieke Wang, and Zhuowen Tu. Open-vocabulary panoptic segmentation with maskclip. *arXiv preprint arXiv:2208.08984*, 2022.
- [12] Mark Everingham, Luc Van Gool, Christopher KI Williams, John Winn, and Andrew Zisserman. The pascal visual object classes (voc) challenge. *International Journal of Computer Vision*, 88:303–338, 2010.
- [13] Golnaz Ghiasi, Xiuye Gu, Yin Cui, and Tsung-Yi Lin. Scaling open-vocabulary image segmentation with image-level labels. In *European Conference on Computer Vision*, pages 540–557, 2022.
- [14] Cong Han, Yujie Zhong, Dengjie Li, Kai Han, and Lin Ma. Zero-shot semantic segmentation with decoupled one-pass network. In *IEEE/CVF International Conference on Computer Vision*, pages 1086–1096, 2023.
- [15] Kunyang Han, Yong Liu, Jun Hao Liew, Henghui Ding, Jiajun Liu, Yitong Wang, Yansong Tang, Yujiu Yang, Jiashi Feng, Yao Zhao, et al. Global knowledge calibration for fast open-vocabulary segmentation. In *IEEE/CVF International Conference on Computer Vision*, pages 797–807, 2023.

- [16] Chao Jia, Yinfei Yang, Ye Xia, Yi-Ting Chen, Zarana Parekh, Hieu Pham, Quoc Le, Yun-Hsuan Sung, Zhen Li, and Tom Duerig. Scaling up visual and vision-language representation learning with noisy text supervision. In *International Conference on Machine Learning*, pages 4904–4916, 2021.
- [17] Siyu Jiao, Yunchao Wei, Yaowei Wang, Yao Zhao, and Humphrey Shi. Learning mask-aware clip representations for zero-shot segmentation. In *Advances in Neural Information Processing Systems*, 2023.
- [18] Siyu Jiao, Hongguang Zhu, Jiannan Huang, Yao Zhao, Yunchao Wei, and Humphrey Shi. Collaborative vision-text representation optimizing for open-vocabulary segmentation. In *European Conference on Computer Vision*, pages 399–416, 2024.
- [19] Dong Jing, Xiaolong He, Yutian Luo, Nanyi Fei, Guoxing Yang, Wei Wei, Huiwen Zhao, and Zhiwu Lu. Fineclip: Self-distilled region-based clip for better fine-grained understanding. *Advances in Neural Information Processing Systems*, 2024.
- [20] Boyi Li, Kilian Q Weinberger, Serge Belongie, Vladlen Koltun, and Rene Ranftl. Language-driven semantic segmentation. In *International Conference on Learning Representations*, pages 1–13, 2022.
- [21] Liunian Harold Li, Mark Yatskar, Da Yin, Cho-Jui Hsieh, and Kai-Wei Chang. Visualbert: A simple and performant baseline for vision and language. *ArXiv*, abs/1908.03557, 2019.
- [22] Feng Liang, Bichen Wu, Xiaoliang Dai, Kunpeng Li, Yinan Zhao, Hang Zhang, Peizhao Zhang, Peter Vajda, and Diana Marculescu. Open-vocabulary semantic segmentation with mask-adapted clip. In *IEEE/CVF Conference on Computer Vision and Pattern Recognition*, pages 7061–7070, 2023.
- [23] Tsung-Yi Lin, Michael Maire, Serge J. Belongie, James Hays, Pietro Perona, Deva Ramanan, Piotr Dollár, and C. Lawrence Zitnick. Microsoft coco: Common objects in context. In *European Conference on Computer Vision*, 2014.
- [24] Fan Liu, Delong Chen, Zhangqingyun Guan, Xiaocong Zhou, Jiale Zhu, Qiaolin Ye, Liyong Fu, and Jun Zhou. Remotecclip: A vision language foundation model for remote sensing. *IEEE Transactions on Geoscience and Remote Sensing*, 2024.
- [25] Haotian Liu, Chunyuan Li, Qingyang Wu, and Yong Jae Lee. Visual instruction tuning. In *Advances in Neural Information Processing Systems*, 2023.
- [26] Yong Liu, Sule Bai, Guanbin Li, Yitong Wang, and Yansong Tang. Open-vocabulary segmentation with semantic-assisted calibration. In *Proceedings of the IEEE/CVF Conference on Computer Vision and Pattern Recognition*, pages 3491–3500, 2024.
- [27] Jiasen Lu, Dhruv Batra, Devi Parikh, and Stefan Lee. Vilbert: Pretraining task-agnostic visiolinguistic representations for vision-and-language tasks. In *Neural Information Processing Systems*, 2019.
- [28] Roozbeh Mottaghi, Xianjie Chen, Xiaobai Liu, Nam-Gyu Cho, Seong-Whan Lee, Sanja Fidler, Raquel Urtasun, and Alan Yuille. The role of context for object detection and semantic segmentation in the wild. In *IEEE/CVF Conference on Computer Vision and Pattern Recognition*, pages 891–898, 2014.
- [29] Jishnu Mukhoti, Tsung-Yu Lin, Omid Poursaeed, Rui Wang, Ashish Shah, Philip HS Torr, and Ser-Nam Lim. Open vocabulary semantic segmentation with patch aligned contrastive learning. In *IEEE/CVF Conference on Computer Vision and Pattern Recognition*, pages 19413–19423, 2023.
- [30] Aditya Prakash, Kashyap Chitta, and Andreas Geiger. Multi-modal fusion transformer for end-to-end autonomous driving. In *Proceedings of the IEEE/CVF conference on computer vision and pattern recognition*, pages 7077–7087, 2021.
- [31] Jie Qin, Jie Wu, Pengxiang Yan, Ming Li, Ren Yuxi, Xuefeng Xiao, Yitong Wang, Rui Wang, Shilei Wen, Xin Pan, et al. Freeseg: Unified, universal and open-vocabulary image segmentation. *arXiv preprint arXiv:2303.17225*, 2023.
- [32] Alec Radford, Jong Wook Kim, Chris Hallacy, Aditya Ramesh, Gabriel Goh, Sandhini Agarwal, Girish Sastry, Amanda Askell, Pamela Mishkin, Jack Clark, et al. Learning transferable visual models from natural language supervision. In *International Conference on Machine Learning*, pages 8748–8763, 2021.
- [33] Nils Reimers and Iryna Gurevych. Making monolingual sentence embeddings multilingual using knowledge distillation. In *Proceedings of the 2020 Conference on Empirical Methods in Natural Language Processing*. Association for Computational Linguistics, 2020.

- [34] Hugo Touvron, Thibaut Lavril, Gautier Izacard, Xavier Martinet, Marie-Anne Lachaux, Timothée Lacroix, Baptiste Rozière, Naman Goyal, Eric Hambro, Faisal Azhar, Aurélien Rodriguez, Armand Joulin, Edouard Grave, and Guillaume Lample. Llama: Open and efficient foundation language models. *ArXiv*, abs/2302.13971, 2023.
- [35] Xudong Wang, Shufan Li, Konstantinos Kallidromitis, Yusuke Kato, Kazuki Kozuka, and Trevor Darrell. Hierarchical open-vocabulary universal image segmentation. *arXiv preprint arXiv:2307.00764*, 2023.
- [36] Zhecheng Wang, Rajanie Prabha, Tianyuan Huang, Jiajun Wu, and Ram Rajagopal. Skyscript: A large and semantically diverse vision-language dataset for remote sensing. In *AAAI Conference on Artificial Intelligence*, 2024.
- [37] Jason Wei, Xuezhi Wang, Dale Schuurmans, Maarten Bosma, Ed H. Chi, F. Xia, Quoc Le, and Denny Zhou. Chain of thought prompting elicits reasoning in large language models. In *Advances in Neural Information Processing Systems*, 2022.
- [38] Jianzong Wu, Xiangtai Li, Shilin Xu, Haobo Yuan, Henghui Ding, Yibo Yang, Xia Li, Jiangning Zhang, Yunhai Tong, Xudong Jiang, et al. Towards open vocabulary learning: A survey. *IEEE Transactions on Pattern Analysis and Machine Intelligence*, 46(7):5092–5113, 2024.
- [39] Yongqin Xian, Subhabrata Choudhury, Yang He, Bernt Schiele, and Zeynep Akata. Semantic projection network for zero-and few-label semantic segmentation. In *IEEE/CVF Conference on Computer Vision and Pattern Recognition*, pages 8256–8265, 2019.
- [40] Bin Xie, Jiale Cao, Jin Xie, Fahad Shahbaz Khan, and Yanwei Pang. Sed: A simple encoder-decoder for open-vocabulary semantic segmentation. In *IEEE/CVF Conference on Computer Vision and Pattern Recognition*, 2024.
- [41] Chunyu Xie, Bin Wang, Fanjing Kong, Jincheng Li, Dawei Liang, Gengshen Zhang, Dawei Leng, and Yuhui Yin. Fg-clip: Fine-grained visual and textual alignment. *arXiv preprint arXiv:2505.05071*, 2025.
- [42] Jiarui Xu, Shalini De Mello, Sifei Liu, Wonmin Byeon, Thomas Breuel, Jan Kautz, and Xiaolong Wang. Groupvit: Semantic segmentation emerges from text supervision. In *IEEE/CVF Conference on Computer Vision and Pattern Recognition*, pages 18134–18144, 2022.
- [43] Jiarui Xu, Sifei Liu, Arash Vahdat, Wonmin Byeon, Xiaolong Wang, and Shalini De Mello. Open-vocabulary panoptic segmentation with text-to-image diffusion models. In *IEEE/CVF Conference on Computer Vision and Pattern Recognition*, pages 2955–2966, 2023.
- [44] Mengde Xu, Zheng Zhang, Fangyun Wei, Han Hu, and Xiang Bai. Side adapter network for open-vocabulary semantic segmentation. In *IEEE/CVF Conference on Computer Vision and Pattern Recognition*, pages 2945–2954, 2023.
- [45] Mengde Xu, Zheng Zhang, Fangyun Wei, Yutong Lin, Yue Cao, Han Hu, and Xiang Bai. A simple baseline for open-vocabulary semantic segmentation with pre-trained vision-language model. In *European Conference on Computer Vision*, pages 736–753, 2022.
- [46] Qwen An Yang, Baosong Yang, Beichen Zhang, Binyuan Hui, Bo Zheng, Bowen Yu, Chengyuan Li, Dayiheng Liu, Fei Huang, Guanting Dong, Haoran Wei, Huan Lin, Jian Yang, Jianhong Tu, Jianwei Zhang, Jianxin Yang, Jiaxin Yang, Jingren Zhou, Junyang Lin, Kai Dang, Keming Lu, Keqin Bao, Kexin Yang, Le Yu, Mei Li, Mingfeng Xue, Pei Zhang, Qin Zhu, Rui Men, Runji Lin, Tianhao Li, Tingyu Xia, Xingzhang Ren, Xuancheng Ren, Yang Fan, Yang Su, Yi-Chao Zhang, Yanyang Wan, Yuqi Liu, Zeyu Cui, Zhenru Zhang, Zihan Qiu, Shanghaoran Quan, and Zekun Wang. Qwen2.5 technical report. *ArXiv*, abs/2412.15115, 2024.
- [47] Shunyu Yao, Dian Yu, Jeffrey Zhao, Izhak Shafran, Thomas L. Griffiths, Yuan Cao, and Karthik Narasimhan. Tree of thoughts: Deliberate problem solving with large language models. In *Advances in Neural Information Processing Systems*, 2023.
- [48] Qihang Yu, Ju He, Xueqing Deng, Xiaohui Shen, and Liang-Chieh Chen. Convolutions die hard: Open-vocabulary segmentation with single frozen convolutional clip. *arXiv preprint arXiv:2308.02487*, 2023.
- [49] Zhuosheng Zhang, Aston Zhang, Mu Li, and Alexander J. Smola. Automatic chain of thought prompting in large language models. In *International Conference on Learning Representations*, 2023.
- [50] Hang Zhao, Xavier Puig, Bolei Zhou, Sanja Fidler, and Antonio Torralba. Open vocabulary scene parsing. In *IEEE/CVF International Conference on Computer Vision*, pages 2002–2010, 2017.

- [51] Theodore Zhao, Yu Gu, Jianwei Yang, Naoto Usuyama, Ho Hin Lee, Sid Kiblawi, Tristan Naumann, Jianfeng Gao, Angela Crabtree, Jacob Abel, et al. A foundation model for joint segmentation, detection and recognition of biomedical objects across nine modalities. *Nature methods*, 22(1):166–176, 2025.
- [52] Bolei Zhou, Hang Zhao, Xavier Puig, Tete Xiao, Sanja Fidler, Adela Barriuso, and Antonio Torralba. Semantic understanding of scenes through the ade20k dataset. *International Journal of Computer Vision*, 127:302–321, 2019.
- [53] Chong Zhou, Chen Change Loy, and Bo Dai. Extract free dense labels from clip. In *European Conference on Computer Vision*, page 696–712, 2022.

A Qualitative Results of Open-Vocabulary Panoptic Sementation

In Fig. 4, we present qualitative comparisons with MAFT+ [18] on open-vocabulary panoptic segmentation. Our method consistently delivers superior performance across most cases. Notably, it demonstrates improved instance-level discrimination. For example, it more accurately identifies ambiguous categories such as *stool*, and small objects like *plates*.

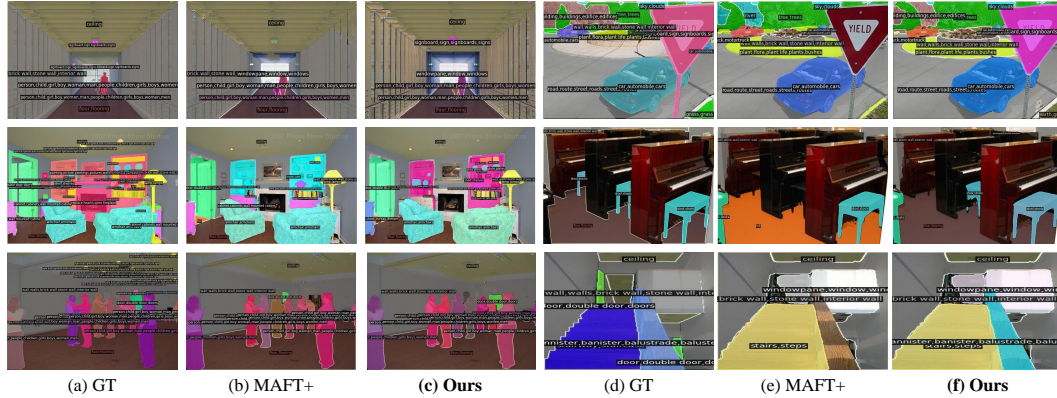


Figure 4: Qualitative comparison with MAFT+ [18] on open-vocabulary panoptic segmentation.

B More Implementation Details

Prompt to LMM We adopt Qwen2.5-VL-72B-Instruct [1] as our Large Multimodal Model (LMM) to generate image-specific reasoning. This model is chosen for its strong instruction-following ability and robust image understanding. Its responses are generally well-structured and coherent, which makes it easier to perform downstream processing and reasoning alignment. We provide the detailed prompts used with Qwen2.5-VL-72B-Instruct [1] to perform step-by-step visual reasoning in our framework. As illustrated in Fig. 5, the reasoning process consists of two components: image-specific reasoning and generic class reasoning. For image-specific reasoning, we guide the LMM through three stages: (1) generating a global image description, (2) identifying candidate classes present in the scene, and (3) producing hierarchical, fine-to-grained reasoning for each observed class. For generic class reasoning—used to supplement missed classes—we similarly apply a three-step process that involves coarse category identification, sub-category refinement, and attribute-based justification. This design ensures that the reasoning output is structured, interpretable, and directly usable for composing descriptive prompts in the segmentation stage. During the use of Qwen2.5-VL-72B-Instruct [1], we set the decoding temperature to 0.7. In a few cases, Qwen2.5-VL-72B-Instruct [1] fails to recognize certain objects in the image despite multiple attempts. For these instances, we discard the image-specific reasoning and rely solely on the generic class reasoning to supplement the segmentation process.

Details of Segmentor As noted earlier, we adopt both SED [40] and MAFT+ [18] as our segmentors. We follow all implementation settings from their respective official releases. Specifically, SED uses 80 segmentation prompts in the prompt composer to predict masks for each category, while MAFT+

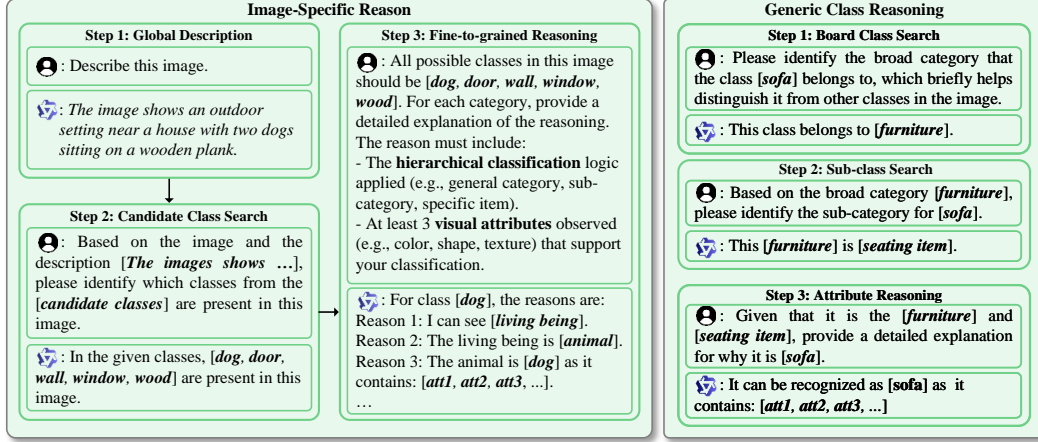


Figure 5: Prompt design for step-by-step visual reasoning. The left panel shows the three-stage process for image-specific reasoning, while the right panel illustrates the prompts of generic class reasoning.

uses 14 prompts. The original prompts follow the format ‘a photo of {c}’, where c denotes the class name. In our method, we enrich these prompts with visual reasoning by appending fine-grained attributes. The modified reason-based format becomes ‘a photo of {c} that has {r}’, where r represents the fine-grained attributes generated by the LMM. We then generate one mask per attribute and apply mask ensembling to produce the final segmentation mask for each class.